







SMPD4 regulates mitotic nuclear envelope dynamics and its loss causes microcephaly and diabetes

 Daphne J. Smits,¹ Rachel Schot,¹ Nathalie Krusy,² Katja Wiegmann,³ Olaf Utermöhlen,³ Monique T. Mulder,⁴ Sandra den Hoedt,⁴ Grace Yoon,⁵  Ashish R. Deshwar,⁵ Christina Kresge,⁶ Beth Pletcher,⁶ Maura van Mook,¹ Marta Serio Ferreira,¹ Raymond A. Poot,⁷ Johan A. Slotman,⁸ Gert-Jan Kremers,⁸ Abeer Ahmad,⁹ Buthaina Albash,¹⁰ Laila Bastaki,¹⁰ Dana Marafi,^{10,11,12} Jordy Dekker,¹  Tjakko J. van Ham,¹ Laurent Nguyen² and  Grazia M. S. Mancini¹

Biallelic loss-of-function variants in *SMPD4* cause a rare and severe neurodevelopmental disorder with progressive congenital microcephaly and early death. *SMPD4* encodes a sphingomyelinase that hydrolyses sphingomyelin into ceramide at neutral pH and can thereby affect membrane lipid homeostasis. *SMPD4* localizes to the membranes of the endoplasmic reticulum and nuclear envelope and interacts with nuclear pore complexes (NPC).

We refine the clinical phenotype of loss-of-function *SMPD4* variants by describing five individuals from three unrelated families with longitudinal data due to prolonged survival. All individuals surviving beyond infancy developed insulin-dependent diabetes, besides presenting with a severe neurodevelopmental disorder and microcephaly, making diabetes one of the most frequent age-dependent non-cerebral abnormalities. We studied the function of *SMPD4* at the cellular and organ levels. Knock-down of *SMPD4* in human neural stem cells causes reduced proliferation rates and prolonged mitosis. Moreover, *SMPD4* depletion results in abnormal nuclear envelope breakdown and reassembly during mitosis and decreased post-mitotic NPC insertion. Fibroblasts from affected individuals show deficient *SMPD4*-specific neutral sphingomyelinase activity, without changing (sub)cellular lipidome fractions, which suggests a local function of *SMPD4* on the nuclear envelope. In embryonic mouse brain, knockdown of *Smpd4* impairs cortical progenitor proliferation and induces premature differentiation by altering the balance between neurogenic and proliferative progenitor cell divisions.

We hypothesize that, in individuals with *SMPD4*-related disease, nuclear envelope bending, which is needed to insert NPCs in the nuclear envelope, is impaired in the absence of *SMPD4* and interferes with cerebral corticogenesis and survival of pancreatic beta cells.

- 1 Department of Clinical Genetics, ErasmusMC University Medical Center Rotterdam, Rotterdam 3015GD, The Netherlands
- 2 GIGA-Stem Cells/Neurosciences, University of Liège, CHU Sart Tilman, B-4000 Liège, Belgium
- 3 Institute for Medical Microbiology, Immunology, and Hygiene, University Hospital Cologne, Center for Molecular Medicine Cologne, University of Cologne, Cologne 50935, Germany
- 4 Department of Internal Medicine, ErasmusMC University Medical Center Rotterdam, Rotterdam, The Netherlands
- 5 Division of Clinical and Metabolic Genetics, Department of Paediatrics, University of Toronto, The Hospital for Sick Children, Toronto, Canada
- 6 Department of Genetics, Rutgers New Jersey Medical School, Newark, NJ, USA

Received September 07, 2022. Revised December 20, 2022. Accepted January 23, 2023. Advance access publication February 3, 2023

© The Author(s) 2023. Published by Oxford University Press on behalf of the Guarantors of Brain.

This is an Open Access article distributed under the terms of the Creative Commons Attribution-NonCommercial License (<https://creativecommons.org/licenses/by-nc/4.0/>), which permits non-commercial re-use, distribution, and reproduction in any medium, provided the original work is properly cited. For commercial re-use, please contact journals.permissions@oup.com

- 7 Department of Cell Biology, ErasmusMC University Medical Center Rotterdam, Rotterdam, The Netherlands
8 Department of Pathology, Optical Imaging Center, ErasmusMC University Medical Center Rotterdam, Rotterdam, The Netherlands
9 Pediatric Endocrinology Unit, Department of Pediatrics, Adan Hospital, Hadiya 52700, Kuwait
10 Department of Pediatrics, Kuwait Medical Genetics Centre, Ministry of Health, Sulaibikhat 80901, Kuwait
11 Section of Child Neurology, Department of Pediatrics, Adan Hospital, Hadiya 52700, Kuwait
12 Department of Pediatrics, Faculty of Medicine, Kuwait University, Safat 13110, Kuwait

Correspondence to: Daphne Jossin Smits
Dr. Molewaterplein 40, 3015 GD Rotterdam, The Netherlands
E-mail: d.smits@erasmusmc.nl

Keywords: SMPD4; microcephaly; insulin-dependent diabetes; nuclear envelope; lipid homeostasis

Introduction

Microcephaly is a rare anomaly defined as a head circumference below -2.5 SD corrected for age and sex, and reflects reduced brain growth during development. Most children born microcephalic (congenital or primary microcephaly) present with a stable disease course, often characterized by (near) normal motor development, mild/moderate intellectual disability and speech disorder. However, another subset of children born with primary microcephaly suffers from a severe disease course with progressive reduction of head circumference, epilepsy, severe developmental delay and early demise. Genetic factors play a major role in the pathogenesis of congenital microcephaly.^{1,2} These factors usually decrease the pool of neuronal progenitors by interfering with neuronal progenitor cell proliferation or survival, during embryonic brain development, which results in decreased brain volume. While many identified genes and pathways related to the cell cycle explain the pathogenesis underlying primary microcephaly with stable course, the factors underlying the progressive disease course are less well-characterized and have been related to abnormal endoplasmic reticulum (ER) stress response and autophagy.³

SMPD4 encodes the enzyme neutral sphingomyelinase-3 and localizes to membranes of the ER and outer nuclear envelope (NE). Neutral sphingomyelinases (SMPD2–5) influence membrane lipid homeostasis by converting sphingomyelin into ceramide and phosphorylcholine. Biallelic variants in SMPD4 have recently been associated with a severe neurodevelopmental syndrome characterized by congenital and progressive microcephaly, epilepsy, congenital arthrogryposis and early demise.^{4–7} Moreover, a few subjects (2/19) also suffered from insulin-dependent diabetes in the first cohort describing SMPD4 loss-of-function (LoF) variants. The association between insulin-dependent diabetes and microcephaly was previously observed in rare recessive microcephalies related to ER stress and apoptosis.^{8–11} Loss of SMPD4 has been shown to affect ER membrane structure by causing dilatation of rough ER cisternae and increased autophagy in patient-derived cells.⁴ However, the effect of SMPD4 loss on the membrane dynamics of the NE and their contribution to human disease is unknown.

The NE is a specialized membrane that consists of two lipid bilayers, the inner and outer nuclear membranes, that separate the nucleus from the cytoplasm. The outer membrane directly derives and holds structural similarities to the rough ER. At sites where the inner and outer nuclear membranes fuse, nuclear pore complexes (NPCs) are embedded in the membrane.^{12,13} NPCs are multiprotein complexes that serve the selective transport of molecules between the nuclear and cytoplasmic compartment.¹⁴ In higher eukaryotes the NE membrane is entirely disassembled and reassembled during

each cell division. During the membrane reassembly, new NPCs are stepwise inserted into the membrane. The formation of a novel NE with properly inserted nuclear pores not only requires strict regulation of membrane expansion, but also needs the induction of membrane curvature.^{15–17} Several membrane-shaping proteins and phosphorylation events are known to regulate membrane dynamics during NE disassembly, reassembly and NPC insertion. However, the regulation of lipid composition and its impact during these processes is still poorly understood.¹⁸

The observation of SMPD4 variants in the pathogenesis of microcephaly offers an unprecedented opportunity to study the function of neutral sphingomyelinases in NE and cell cycle dynamics during brain development. In this study, we expand the knowledge of SMPD4-related disease by describing five previously unreported affected individuals with prolonged survival, who had microcephaly and developed insulin-dependent diabetes in childhood. We used both *in vitro* and *in vivo* systems to gain insight into the function of SMPD4 in NE dynamics and in the developing brain cortex.

Materials and methods

Study approval

The study was approved by the local Institutional Review Board (Erasmus MC Rotterdam, protocol METC-2012387).

Consenting of human subjects

Written informed consent for participation in the study and scientific publication of analysed data and clinical photographs was obtained. GeneMatcher was used to recruit additional previously unreported subjects with biallelic SMPD4 variants and connect with clinicians of previously published subjects for longitudinal and follow-up phenotypic data when available.¹⁹

Mice

All mice were handled according to the ethical guidelines of the Belgian Ministry of Agriculture in agreement with European Community Laboratory Animal Care and Use Regulations (86/609/CEE, Journal Officiel des Communautés Européennes, L358, 18 December 1986). All mice were wild-type (WT) SWISS pregnant females purchased from Janvier Labs and were housed under standard conditions (animals were bred in-house and maintained with *ad libitum* access to food and constant temperature (19–22°C) and humidity (40%–50%) under a 7 a.m. to 7 p.m. light/dark cycle).

Exome sequencing methods

Exome sequencing (ES) was performed on DNA isolated from blood from probands and family members, as previously described.²⁰ ES data are deposited in each medical institute, with respect for the privacy of the families. Details of sequencing and analysis pipelines are described for each family in the [Supplementary material](#).

Statistics

All statistical tests were performed with Prism GraphPad 9 Software. All datasets were tested for outliers and normality. All error bars represent the SEM. P-values <0.05 were considered significant. Details about the statistical tests are available in the figure legends.

Data availability

ES data are deposited at each medical institute referring the individuals, in respect to the privacy of the families.

Results

Undescribed cases with variants in *SMPD4* present with microcephaly and insulin-dependent diabetes

Biallelic variants in *SMPD4* have been described in 25 affected children from 16 unrelated families over the past few years.^{4–7} We expand the phenotype related to *SMPD4* variants by describing the first three adult subjects and presenting two new paediatric cases with additional clinical features. In addition, we provide longitudinal follow-up data on a previously published case. Extensive clinical reports and detailed descriptions of the identified variants are available in the [Supplementary material](#) and [Supplementary Table 3](#). Lastly, we provide a summary of the clinical features observed in all published cases with biallelic *SMPD4* variants ([Table 1](#)).

Family 1

The individuals from this consanguineous family are the first reported adults with *SMPD4* variants ([Fig. 1A](#)). The family consists of three affected daughters, aged 45, 43 and 41 years. At the last examination, all individuals present with microcephaly (−4/−5 SD), short stature and moderate to severe intellectual disability (IQ range: 20–40). All three sisters were reported with ataxia and tremors. Joint contractures were not noted. Interestingly, all sisters developed insulin-dependent diabetes during their teenage years. Two of them also presented with retinal dystrophy and hearing loss. They started walking at 2 years of age. As this family consulted the genetics clinic for the first time at adult age, extensive information about their perinatal/paediatric features is unavailable. Exome sequencing revealed a homozygous missense variant in *SMPD4* in all three affected daughters [NM_01751.4(*SMPD4*):c.2431C>T p.(Arg811Cys)]. This variant has a very low minor allele frequency in gnomAD (0.0022%) and is absent in homozygous state in gnomAD controls. This variant was predicted to be deleterious by SIFT, probably damaging by PolyPhen-2 and benign by MutationTaster. Both parents were heterozygous carriers of the variant and their healthy son is wild-type.

Family 2

The second family includes one affected child born with congenital bilateral talipes equinovarus. He was reported to be borderline

microcephalic (−2 SD), hypotonic and delayed in all domains of development at 1 year of age. At the age of 5 years, he developed additional contractures of both knees and hips. This boy was diagnosed with insulin-dependent diabetes at the age of 15 years. A brain MRI was completed at age 11 years, which revealed diffuse simplification of the gyral pattern, thickening of the cerebral cortex, a thin corpus callosum and decreased volume of the cerebellar vermis ([Fig. 1B–D](#)). Trio exome sequencing revealed a homozygous single basepair deletion in *SMPD4*. The variant is denoted as c.940delT and results in a frameshift and creation of a premature stop codon [NM_01751.4(*SMPD4*):c.940delT p.(Ser314Profs*60)]. Both parents were confirmed to be heterozygous carriers of the variant. To study the effect of this variant on *SMPD4* expression, RNA was isolated from primary fibroblasts of the affected proband. Quantitative reverse transcriptase-PCR (RT-PCR) indicates that the expression of *SMPD4* is 80% reduced in patient-derived cells, confirming the pathogenicity of this variant ([Supplementary Fig. 1A](#)).

Family 3

After the original report (Family 8 in Magini et al.⁴), a new sibling was born in this family and follow-up was recorded. Currently, this family consists of three affected children born from consanguineous parents. One of these siblings (Family 3 Subject VI-2; [Fig. 1E](#)) was previously described in Magini et al.⁴ During infancy this subject presented with respiratory failure, severe microcephaly (−6 SD), arthrogryposis, generalized seizures, vocal cord paralysis, feeding intolerance, hypertonia, intermittent sinus bradycardia and persistent foramen ovale. In this individual, a homozygous nonsense variant was identified [NM_01751.4(*SMPD4*): c.370G>T; p.(Glu124*)]. Follow-up at 5 years of age revealed several additional features, including insulin-dependent diabetes, focal segmental glomerulosclerosis and retinal dystrophy. The same variant was identified in the newborn sibling in this family (Family 3 Subject VI-3; [Fig. 1F and G](#)). This subject presented with a similar disease course including persistent respiratory failure, generalized seizures, severe progressive microcephaly (−6 SD), distal arthrogryposis and severe global developmental delay. Like his brother, this sibling developed type 1 diabetes at 4 years of age. In addition, he showed long QT syndrome, chorea and dyskinesia of the tongue. A third sibling in this family (Family 3 Subject VI-1), who presented with similar features, died *in utero* in the seventh month of the pregnancy.

Summary of the *SMPD4*-related phenotype

Following on from our cohort published in 2019, additional individuals harbouring variants in *SMPD4* have been described.^{4–7} Most of these individuals presented with microcephaly, arthrogryposis and severe neurodevelopmental delay. [Table 1](#) provides a summary of all features observed in all described *SMPD4* cases ($n = 30$), including the novel cases presented in this study. This summary shows that intrauterine growth retardation (IUGR), microcephaly at birth, arthrogryposis and severe developmental delay are the most prevalent features. The microcephaly had a progressive character in almost all subjects for whom follow-up data were available (85%). On the other hand, few cases were reported with normal occipital frontal circumference (OFC) measurements at birth, but developed microcephaly later on. Another frequently observed manifestation in this cohort is neonatal respiratory distress (73%). This feature was mainly observed in severely affected individuals and is the most frequently reported cause of death in infancy.

Table 1 Summary of the clinical features observed in all described individuals with SMPD4 variants

Disease manifestation	Number of individuals with biallelic SMPD4 variants ^a (n = 30)	% of all assessed individuals
Growth parameters and survival		
IUGR	15/24	62.5
Congenital microcephaly	19/26	73.1
Length < -2.5 SD at birth	6/12	50.0
Prematurity	10/22	45.5
Death in infancy (<1 year of age)	9/27	33.3
Neonatal respiratory distress	16/22	72.7
Neurological abnormalities		
Progressive microcephaly ^b	11/13	85.0
Seizures	14/25	56.0
Persistent respiratory distress	12/25	48.0
Congenital arthrogryposis	23/30	76.6
Developmental delay	15/15	100.0
Facial dysmorphisms	20/20	100.0
Brain MRI		
Simplified gyration	17/23	73.9
Thin corpus callosum	13/24	54.2
Hypomyelination	11/23	47.8
Cerebellar hypoplasia	11/24	45.8
Brainstem hypoplasia	5/24	20.8
Thickening of the cortex	1/24	4.2
Non-neurological systemic abnormalities		
Congenital heart defect	11/25	44.0
Atrial septum defect	4/25	16.0
Persistent ductus arteriosus	5/25	20.0
Long QT	1/25	4.0
Dilated cardiomyopathy	1/25	4.0
Ventricular septum defect	2/25	8.0
Transposition of great arteries	1/25	4.0
Insulin-dependent diabetes	7/26 (age of onset between 3 and 14 years)	27.0
Ocular anomalies:	5/17 (17 ophthalmologist report available)	29.4
Retinopathy	3/17	17.6
Macular dystrophy	1/17	5.9
Faint corneal opacity	1/17	5.9
Renal disease:	3/11 (for 11 renal ultrasound was available)	27.8
Focal segmental glomerulosclerosis	1/11	9.1
Mild pyelectasis	1/11	9.1
Multicystic dysplastic kidney	1/11	9.1
Muscular tone		
Hypotonic	5/19	26.3
Hypertonic	12/19	63.2
Normotonic	2/19	10.5

IUGR = intrauterine growth retardation.

^aThe number of individuals with SMPD4 variants for which detailed clinical information was available.

^bDefined as >0.5 SD occipital frontal circumference (OFC) decline after birth.

Besides the core phenotypic features, additional features were observed in the new cases. First, we observed a remarkable increase in individuals that present with insulin-dependent diabetes (27%). This observation was frequently made in individuals who survived beyond infancy. The age of diabetes onset was between 3 and 15 years of age, and if reported these children were negative for anti-insulin, anti-glutamic acid decarboxylase (anti-GAD) and anti-islet antigen 2 (anti-IA2) antibodies. Moreover, individuals from three families presented with visual defects reported as retinal dystrophy, macular dystrophy, retinal pigment epithelial stippling and nystagmus. Lastly, several cardiac defects were described in addition to the previously reported hypertrophic cardiomyopathy. These defects included persistent ductus arteriosus, persistent foramen ovale and long QT syndrome, but each has been sporadically reported. From this observation, the only consistent and frequent

feature, besides the neurological abnormalities, seems to be insulin-dependent diabetes, with childhood onset.

SMPD4 pathogenic variants

In total, 19 unique intragenic variants in SMPD4 are described, of which five are missense variants, four are nonsense variants, five are splice site variants predicted to result in a frameshift, four are confirmed frameshift variants and one is a genomic deletion including exons 18–20 of SMPD4. In addition, two bigger genomic deletions including SMPD4 were described. The missense variants are spread over the entire protein structure (Fig. 1H). All variants, including the missense, are absent or have a very low frequency in control cohorts and are predicted to have deleterious effects on protein functioning. An overview of all described pathogenic variants

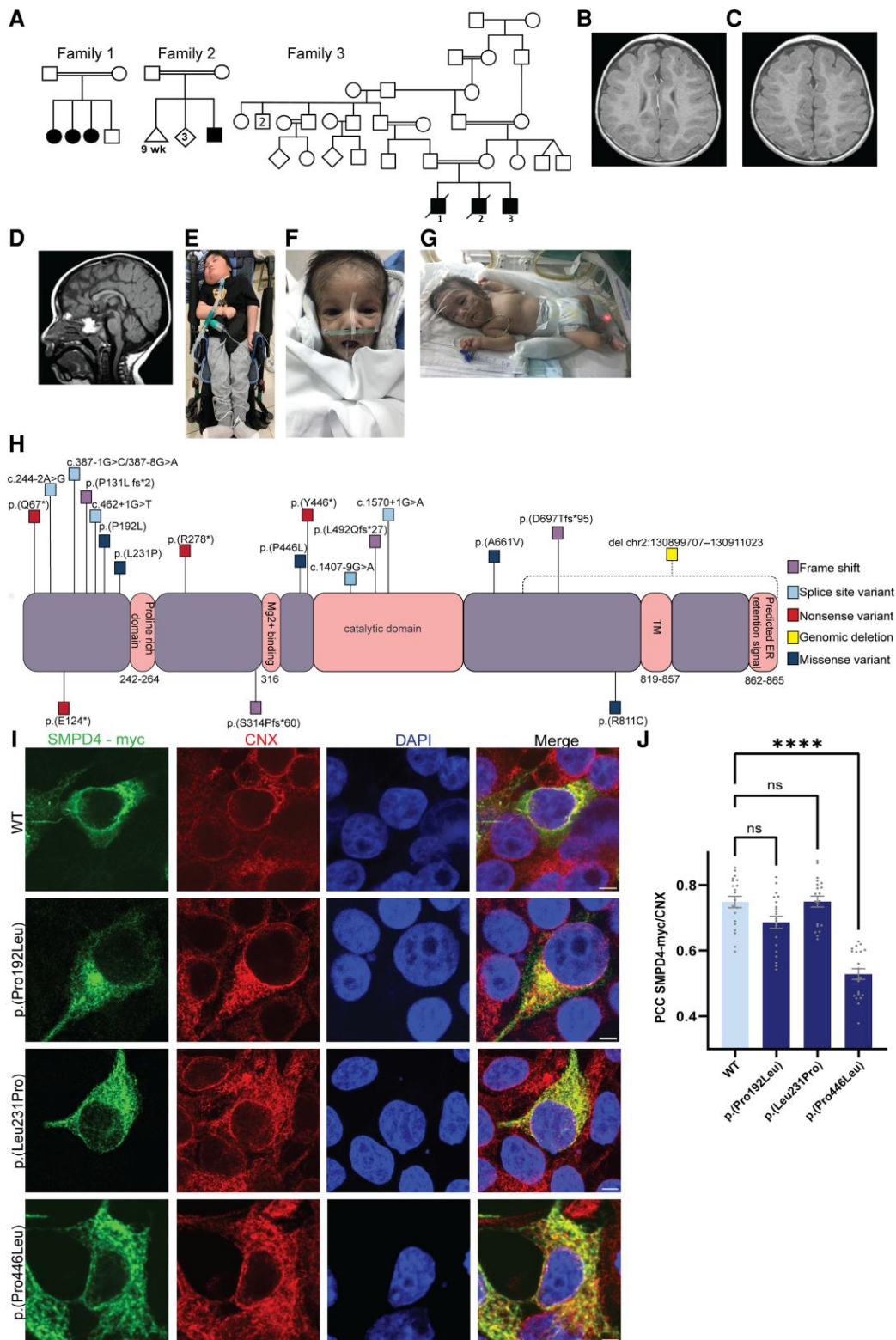


Figure 1 Clinical phenotype and SMPD4 variants. (A) Pedigrees of the three described families. Affected individuals are indicated with filled symbols. (B–D) Brain MRI of the affected Subject II-3 Family 2, at 11 years of age. T₁-weighted images show simplified gyration, thickening of the cortex (B and C), thin corpus callosum (D) and reduced volume of the cerebellar vermis (D). (E–G) Facial features of affected Subjects 2 (E) and 3 (F and G) from Family 3. (H) Schematic overview of the SMPD4 protein structure, the known protein domains and all identified intragenic pathogenic variants. New variants described in this manuscript are depicted below the protein structure. Previously described variants are depicted above the protein structure. (I) Subcellular localization of the SMPD4 proteins containing missense variants Pro192Leu, Leu231Pro, Pro446Leu in HEK293T cells. Samples were costained with the ER marker anti-calnexin (CNX, green) and anti-myc (red) and DAPI (blue). Scale bars = 5 μm. (J) Co-localization of SMPD4-mutant proteins with CNX was determined by calculating Pearson's correlation coefficient (Kruskal-Wallis test, n = >20 cells per group, n = 3 experiments, P = <0.0001).

in SMPD4 and their frequency is provided in [Supplementary Table 4](#). To assess the pathogenic mechanisms of SMPD4 missense variants we introduced the previously reported variants p.(Leu446Pro), p.(Pro231Leu) and p.(Pro192Leu) into a human Myc-tagged SMPD4 plasmid.^{4,5} These plasmids were transiently transfected in HEK293T cells and the proteins were followed by co-localization studies with markers of the ER and NPC by confocal microscopy. All mutants showed localization to the ER and the NE/NPC, similar as the wild-type protein ([Fig. 1I](#) and [Supplementary Fig. 1B](#)). However, the mutant p.(Pro446Leu) (Pearson's correlation coefficient = 0.53) showed less co-localization with the ER membrane marker calnexin, as compared to wild-type SMPD4 (Pearson's correlation coefficient = 0.75) and the mutants p.(Pro192Leu) (Pearson's correlation coefficient = 0.67) and p.(Pro231Leu) (Pearson's correlation coefficient = 0.75; [Fig. 1I](#)). In addition, overexpression of p.(Pro446Leu) seemed to affect the calnexin distribution ([Fig. 1J](#)). These data show that the variants do not induce major alterations in the localization patterns, although one shows reduced localization to the ER.

SMPD4 loss affects cell division and apoptosis in human neural stem cells

Congenital microcephaly is often caused by a decrease number in neuronal progenitor that followed their impaired proliferation rates, e.g. DNA synthesis and mitotic defects, or their increased cell death.^{1,2} We have previously demonstrated that primary fibroblasts from individuals expressing LoF variants in SMPD4 show defects in cell division and are more susceptible to undergo apoptosis.⁴

In order to gain insight in the effects of SMPD4 depletion on neural cell lineages, cell proliferation and apoptosis were investigated in human neural stem cells (hNSCs). These pluripotent stem cells can be used as surrogate of precursors of neuronal and glial progenitors, and hence are a good model for a proliferation defect. First, the proliferating capacities of hNSCs were assessed by measuring 5-ethynyl-2'-deoxyuridine (EdU) incorporation after knockdown of SMPD4 with siRNAs (siSMPD4; [Fig. 2A](#) and [Supplementary Fig. 1C](#)). Lipofection of siSMPD4 led to a significant decrease in EdU-positive cells compared to treatment with siCTRL ([Fig. 2B](#); siCTRL: 55.5%, siSMPD4: 34.2%). Afterwards, susceptibility of siSMPD4-treated hNSCs to undergo apoptosis was investigated by detecting apoptotic DNA fragments after stress induction with 0.1 mM hydrogen peroxide treatment. hNSCs expressing siSMPD4 showed a significant increase in cells with apoptotic foci (46%) as compared to controls (30.8%; [Supplementary Fig. 1D and E](#)). These data confirm that the increased susceptibility to apoptosis observed in native fibroblasts from affected individuals results from SMPD4 depletion and demonstrates that SMPD4 is essential to maintain proliferating capacities and cell survival in neuronal lineages.

Cell cycle duration in SMPD4-depleted cells

The impact of SMPD4 depletion on the cell cycle was further investigated by real-time live imaging of fibroblasts from individuals with LoF SMPD4 variants and hNSCs treated with siSMPD4. Fibroblasts with LoF variants in SMPD4 showed a prolonged mitosis without morphological abnormalities during cell division as compared to controls. The observed average mitotic duration in SMPD4-depleted fibroblasts was 1.22 times longer as compared to controls ([Fig. 2C–E](#) and [Supplementary Videos 1 and 2](#); controls:

58 min; SMPD4 LoF variant: 71 min). The effect of SMPD4 depletion on mitotic duration was confirmed in hNSCs, as the average mitotic duration increased 1.47 times after siSMPD4 treatment ([Fig. 2F](#) and [Supplementary Videos 3 and 4](#); siCTRL: 38 min; siSMPD4: 56 min). The contribution of morphological abnormalities to the increased mitotic duration was evaluated in more detail. We evaluated bipolar spindle formation, chromosome (mis)segregation and spindle length in fibroblast and mitotic ER localization upon siSMPD4 in HEK293T cells but did not observe any overt differences during these processes ([Supplementary Fig. 2A–C](#)).

SMPD4 depletion disrupts nSMase3 activity without changing (sub)cellular lipidome fractions

Although SMPD4 (also named nSMase-3) has been shown to have neutral sphingomyelinase activity, there are no reports about its enzymatic activity in native human cells.²¹ We investigated sphingosine-phosphodiesterase activity of cultured fibroblasts of affected individuals using ¹⁴C-labelled sphingomyelin at neutral pH, according to Quintern and Sandhoff.²² SMPD4-specific sphingomyelinase activity was elicited by treatment with tumor necrosis factor α (TNF α), in order to distinguish it from other neutral sphingomyelinases, as previously described.²³ Cell homogenates derived from unrelated affected subjects with complete SMPD4 LoF variants (Families 1 and 2 from Magini *et al.*⁴) already showed decreased sphingomyelinase activity and no induction of its activity upon TNF α treatment. TNF α treatment of SMPD4 LoF cells did not promote induction of enzymatic activity while the control cells did show a clear response ([Fig. 2G](#)). This demonstrates that the human mutations impair the neutral sphingomyelinase activity in cultured fibroblasts and confirm that SMPD4 is a TNF α -dependent neutral sphingomyelinase.

In fibroblasts and HEK293T cells, SMPD4 localizes to the NE membrane and interacts with several NPC components. Therefore, we evaluated the effect of SMPD4 depletion on the lipid composition of the nuclear membrane. Nuclear-enriched fractions were isolated from fibroblasts of individuals with SMPD4 LoF variants and control fibroblasts for lipidomic analysis. The purity of the nuclear fractions was confirmed with immunoblots probing the nuclear marker lamina-associated polypeptide-2 (LAP2; [Supplementary Fig. 3A](#)). Several sphingolipid subtypes were quantified, including sphingomyelin, ceramide and sphingosine 1 phosphate (S1P). Fibroblasts derived from individuals with LoF variants in SMPD4 did not show any alteration in sphingomyelin or ceramide levels when compared to several control fibroblast lines ([Fig. 2H and I](#)). S1P levels were below the limit of detection in all samples and therefore could not be determined accurately. This demonstrates that SMPD4 is probably not the major neutral sphingomyelinase in cultured cells controlling the global sphingolipid/ceramide pool of nuclear membranes, but may have a specific local effect on the NPC membrane. Therefore, we focused on aspects of NPC morphology and NE dynamics.

SMPD4 regulates nuclear envelope dynamics and nuclear pore complex insertion

The morphology of the NE was examined to evaluate the effect of SMPD4 deficiency on the membrane structure. The NE morphology was first studied on fixed fibroblasts with the NE marker LAP2. Alterations in NE morphology were observed in fibroblasts derived from three unrelated affected individuals ([Supplementary Fig. 3B](#)). These cell lines showed an increased number of invaginations from the inner nuclear membrane into the nucleoplasm (21.3%),

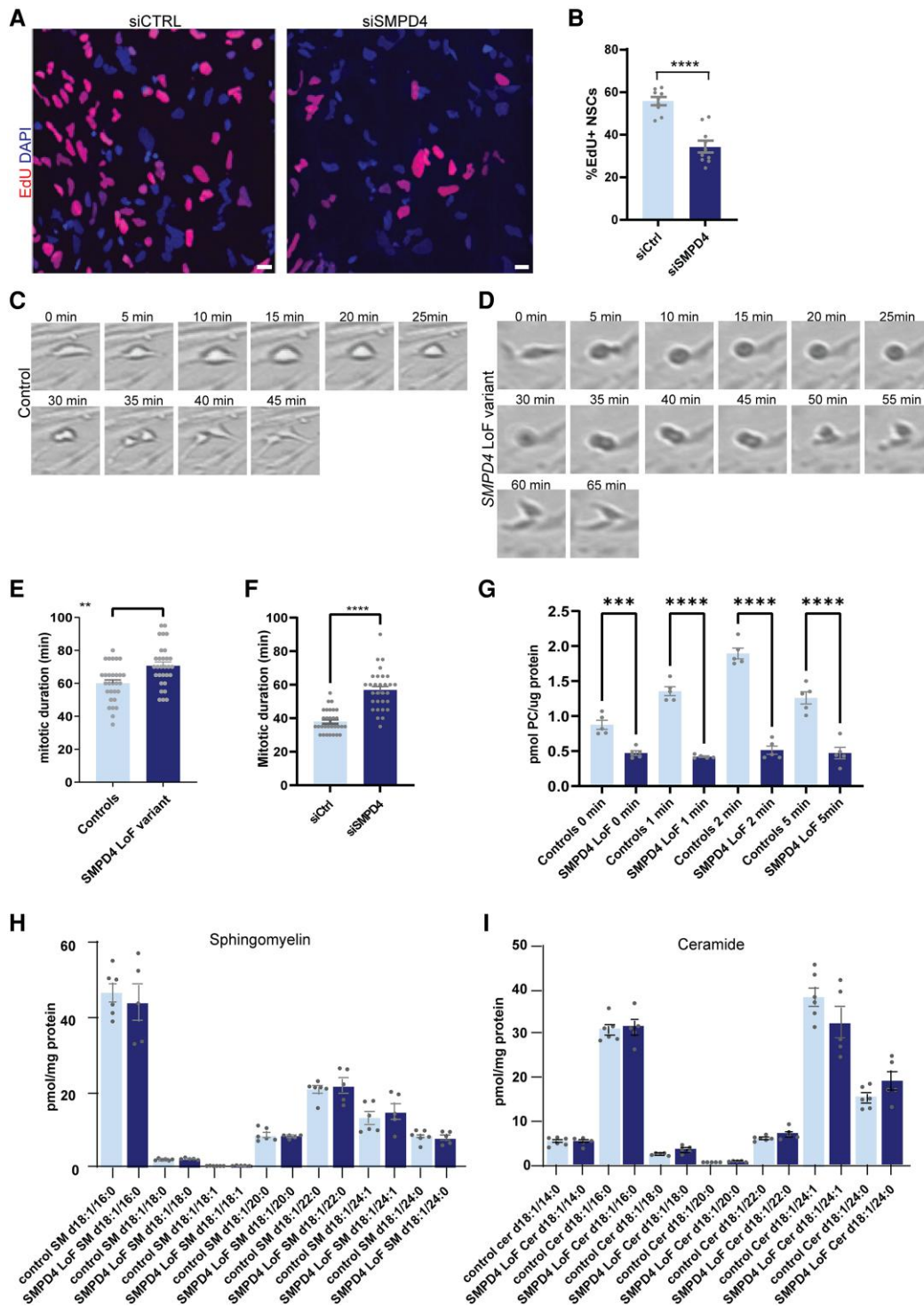


Figure 2 SMPD4 depletion disturbs cell cycle progression and reduces nSMase activity. (A) The Click-IT EdU proliferation assay was performed on hNSCs 48 h after siSMPD4 or siCTRL transfections. Cells that did incorporate EdU during incubation are shown in lighter colour (red), all nuclei were counterstained with DAPI. Scale bars = 10 μ m. (B) Quantification of the percentage of proliferating hNSCs. The number of EdU⁺ cells was calculated as a percentage of all DAPI⁺ nuclei (unpaired t-test with Welch's correction, two-tailed, $n > 5$ fields per slide, $P = < 0.0001$). (C and D) Time-lapse brightfield microscopic imaging of human control fibroblasts (C) and fibroblasts harbouring LoF SMPD4 variants (D, Family 1 from Magini et al.⁴). (E) Quantification of the mitotic duration observed in C and D ($n = 2$ cell lines with SMPD4 LoF variants: Families 1 and 2 from Magini et al.,⁴ $n = 3$ control cell lines, unpaired t-test, two-tailed, $P = 0.0014$). (F) Quantification of the time-lapse brightfield microscopic imaging of human NSCs treated for 48 h with siSMPD4 or siCTRL siRNAs ($n = 3$ experiments, unpaired t-test with Welch's correction, two-tailed, $P = < 0.0001$). (G) nSMase enzymatic activity assay. Fibroblasts were treated with TNF α to induce nSMase-3 activity after which the production of radioactive phosphor-ylcholine produced from ¹⁴C-SM was quantified ($n = 2-3$ experiments, $n = 2$ cell lines with SMPD4 LoF variants: Families 1 and 2 from Magini et al.,⁴ $n = 2$ control cell lines, one-way ANOVA with Sidák post hoc test, *** $P = 0.0004$, **** $P = < 0.0001$). (H and I) Tandem mass spectrometry (MS/MS) profiling sphingomyelin (SM, H) and ceramide (Cer, I) subtypes in nuclear fractions of control fibroblasts and fibroblasts harbouring LoF SMPD4 variants. Cer and SM subtypes were distinguished based on their fatty acyl chain length ($n = 1$ experiment, $n = 2$ control cell lines, $n = 2$ cell lines with SMPD4 LoF variants: Families 1 and 2 from Magini et al.⁴).

compared to control cell lines (9.9%; [Supplementary Fig. 3B–D](#)). As these invaginations can be a normal feature during mitotic NE breakdown and reassembly, live NE dynamics were studied by live-imaging of overexpressed lamin B receptor (LBR)–green fluorescent protein (GFP) marker, in HEK293T cells after SMPD4 knockdown.

Before the onset of mitosis, NE-associated dynein generates pulling forces on microtubules that emanate from the centrosomes. These pulling forces lead to the formation of NE invaginations around centrosomes in prophase and facilitate NE disassembly.¹⁵ In siCTRL-treated cells, the formation of these NE invaginations was almost immediately followed by complete disassembly of the NE and progression into metaphase ([Supplementary Video 5](#)). Instead, siSMPD4-treated cells showed a significant delay between the formation of these invaginations, membrane disassembly and metaphase in independent biological replicates (siCTRL: 33.6 min, siSMPD4: 60.0 min). The time span from metaphase until the onset of NE rebuilding was similar in both groups. Following chromatin separation, siSMPD4 cells did start reassembly of the novel NE in late anaphase, similar to siCTRL-treated cells. However, in the absence of SMPD4, the subsequent closure and expansion of the NE resulted in polylobed membrane structures and a significant delay in the formation of a closed NE ([Fig. 3A and B](#); siCTRL: 40.2 min, siSMPD4: 70.1 min). During interphase, nuclei of siSMPD4-treated cells did not show increased infoldings, which suggests that the invaginations seen with LAP2 antibodies on fixed sections are related to NE membrane remodelling events during mitosis. These results correlate SMPD4's neutral sphingomyelinase activity specifically to the NE assembly during mitosis.

During NE reassembly, large numbers of NPCs have to be inserted in the new NE. To assess the effect of altered NE membrane structure on NPC insertion, we counted NPC numbers. Three-dimensional structured illumination microscopy (3D SIM) was used to identify NPCs labelled with the mAb414 antibody, which recognizes phenylalanine–glycine (FG) repeat-containing NPCs. Initially, NPC numbers were counted in all cell-cycle phases. Fibroblasts derived from unrelated individuals with SMPD4 variants showed a significantly decreased number of NPCs per nuclear surface area ([Fig. 3C and Supplementary Fig. 3E](#); Controls: 4.87 pore/ μm^2 ; SMPD4 LoF variants: 3.99 pore/ μm^2). As NPC assembly can occur in the post-mitotic phase and during interphase, we used the post-mitotic marker CDT1 and late G2 marker CyclinB to discriminate between these two processes. Fibroblasts derived from unrelated patients with SMPD4 variants contained fewer nuclear pores per nuclear surface area in both post-mitotic conditions ([Fig. 3D](#)) and during interphase ([Fig. 3E](#); Controls: 4.28 pore/ μm^2 ; SMPD4 LoF variants: 3.6 pore/ μm^2). These data show that SMPD4 disruption not only delays post-mitotic NE membrane assembly, but also alters post-mitotic NPC assembly. To obtain additional evidence for a role of SMPD4 in post-mitotic NPC biogenesis, we used RNAi to knockdown SMPD4 in hNSCs and counted NPCs in CDT1-positive cells. In SMPD4-depleted hNSCs we observed a decrease of NPCs per nuclear surface area ([Fig. 3F](#); siCTRL: 4.4 pore/ μm^2 , siSMPD4: 3.6 pore/ μm^2). Altogether, these data showed that depletion of SMPD4 interferes with the NE dynamics during mitosis, which is compatible with impaired post-mitotic insertion of NPCs.

SMPD4-GFP localizes to pericentrosomal regions during mitosis

SMPD4 activity does not alter global sphingolipid pool, but regulates NE assembly. We thus hypothesize that its function might relate

to its subcellular localization. To test this we followed SMPD4 localization during mitosis with live confocal imaging. Human SMPD4 was subcloned into a pEGFP-C1 vector. As expected, SMPD4-GFP-C1 localized to the NE and ER in interphase after transient overexpression in HEK293T cells ([Supplementary Fig. 4A](#)). In addition, co-precipitation of SMPD4-GFP with NUP153 and NUP62 was observed, confirming close association with NPCs ([Supplementary Fig. 4B and C](#)). At the onset of mitosis (early prophase) SMPD4-GFP accumulated at one site near the nuclear rim ([Supplementary Video 6](#)). This strong signal was subsequently split into two signals, which both localized to sites of mitotic NE invagination. These findings suggested the enrichment of SMPD4 to regions surrounding the centrosomes during the onset of mitosis. To confirm this observation, we performed co-stainings of SMPD4-GFP with the centrosomal marker γ -tubulin ([Fig. 4A](#)). We observed a localization of SMPD4 to pericentriolar regions during all mitotic stages. However, this co-localization was most pronounced during (early) prophase.

The formation of a new NE around chromatin starts in late anaphase. As major defects were observed in NE reassembly and NPC insertion upon SMPD4 depletion, we assessed the localization of SMPD4-GFP to chromatin surrounding during these processes. We observed localization of SMPD4 to the vicinity of chromatin after cell division ([Fig. 4A and B](#)). Co-stainings with the nuclear pore marker 414 showed that SMPD4 punctae in these phases localize together with NPC marker.

SMPD4 loss decreases cortical progenitor proliferation and alters their fate

We next tested whether SMPD4 is also required for the proliferation of the apical progenitors that reside in the ventricular zone (VZ) and that generate projection neurons during embryogenesis. We thus depleted *Smpd4* in apical progenitors from embryonic Day 14.5 (E14.5) mice by *in utero* electroporation of two validated small hairpin (sh)RNAs targeting *Smpd4*, referred to as *Smpd4_A* and *Smpd4_B* ([Supplementary Fig. 5A and B](#)). This was followed 2 days later by a single injection of EdU (50 mg/kg) in pregnant dams 1 h before sacrifice of the embryos to label cortical cells undergoing S-phase. We determined the proliferation rate (cell undergoing mitosis) by quantifying the percentage of EdU+ cells in apical progenitors (SOX2⁺) that were targeted by electroporation (GFP⁺) [ratio of SOX2⁺ + GFP⁺ + EdU⁺ / (SOX2⁺ + GFP⁺) × 100%]. Apical progenitors transfected with the shSMPD4 vectors showed a reduction in proliferation rate as compared to those targeted with the shCtrl ([Fig. 5A and B](#) shCtrl: 43%; shSMPD4_A: 23%; shSMPD4_B 28%). We next tested whether the reduction of proliferation rate observed upon depletion of SMPD4 was correlated with an increase of cell-cycle exit. For this purpose, embryos were electroporated at E14.5, then injected with EdU (50 mg/kg) at E15.5 and finally sacrificed 20 h later (E16.5) for analysis. The fraction of progenitors that did exit the cell cycle (Ki67⁻) upon proliferation in the last 20 h was quantified [Ki67⁻ + GFP⁺ + EdU⁺ / (EdU⁺ + GFP⁺) × 100%; [Fig. 5C and Supplementary Fig. 5C](#)] and showed that the downregulation of SMPD4 in apical progenitors led to an increase in cell cycle exit (shSmpd4_A/B: 50%), as compared to shCtrl-targeted apical progenitors (shCtrl 41%).

To assess whether the promotion of cell-cycle exit upon depletion of *Smpd4* resulted in an increased neuronal output, we quantified the proportion of newborn expression of the neuronal marker β IIIITubulin [β IIIITub⁺ + GFP⁺ + EdU⁺ / (EdU⁺ + GFP⁺) × 100%]. ShSMPD4-targeted cells showed an increase in

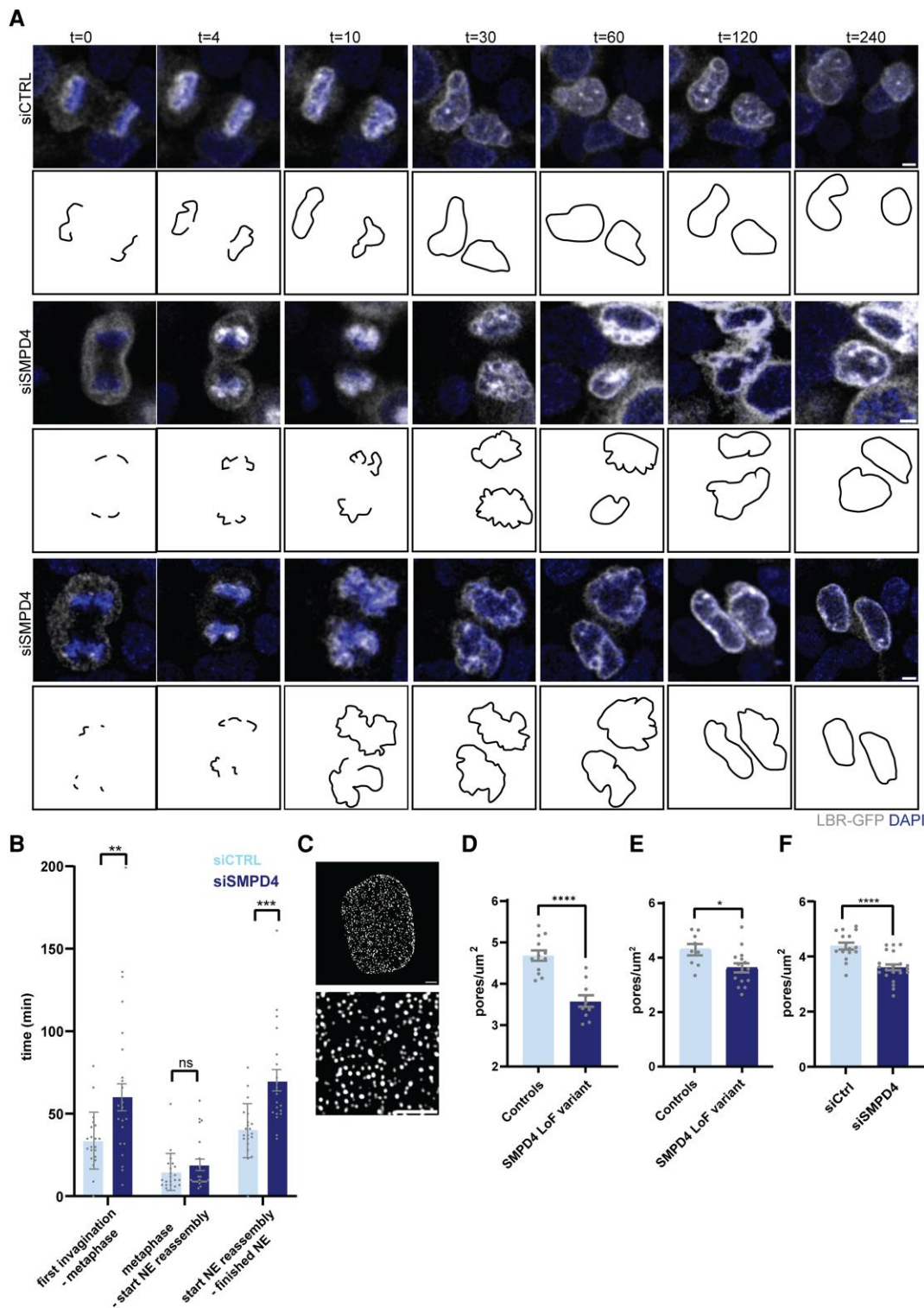


Figure 3 SMPD4 regulates NE membrane structure and NPC insertion. (A) Live HEK293T-cells expressing exogenous lamin B receptor–GFP were imaged during mitosis 72 h after siRNA transfection with siSMPD4 or siCTRL. The periods of NE reassembly were defined as: the first frame in which NE invaginations were visible until the first frame of metaphase; metaphase until the first frame of visible NE reassembly; the first frame of visible NE reassembly until a closed rounded NE without the presence of irregularities. The lower panels show outlines of the developing NE structure. (B) Quantification of A, showing the duration of each mitotic phase in minutes (one-way ANOVA with Sidák post hoc test, $n > 50$ cells per group, ** $P = 0.0022$, *** $P = 0.0005$). (C) 3D SIM super resolution images showing FG-repeat containing nuclear pores (anti-mab414) in control fibroblast. (D and E) Fibroblasts were counterstained with cell-cycle markers CDT1 (D, post-mitotic phase) or cyclinB1 (E, G2-phase). The number of mab414⁺ nuclear pores per μm^2 was counted in CDT1/CyclinB1-positive cells with 3D SIM high-resolution microscopy [$n = 2$ –3 experiments, unpaired t-test, two-tailed, $P < 0.0001$ (D), $P = 0.019$ (E), scale bars = 1 μm]. (F) The number of nuclear pores (anti-mab414) was quantified in hNSCs treated for 48 h with siSMPD4 or siCTRL siRNAs. hNSCs were costained with the CDT1 antibody to visualize post-mitotic cells ($n = 2$ experiments, unpaired t-test with Welch’s correction, two-tailed, $P < 0.0001$).

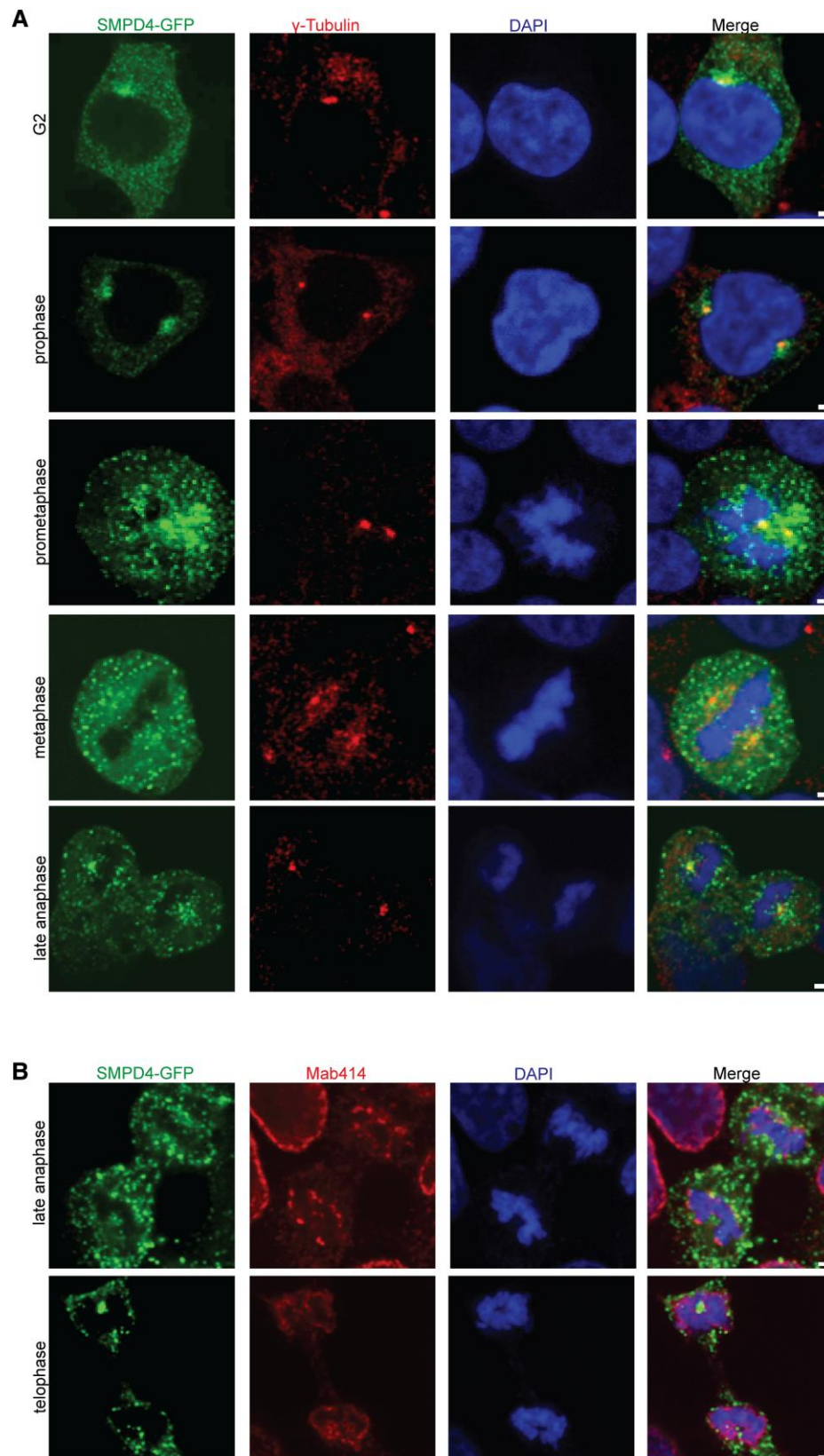


Figure 4 SMPD4-GFP localizes to pericentriolar regions during mitosis. (A) Fluorescent confocal images showing SMPD4-GFP-C1 (first column, green) localization in mitotic HEK293T cells during different stages of cell division. Antibodies against γ -tubulin (second column, red) were used to visualize centrosomes. Nuclei were counterstained with DAPI (third column, blue). (B) Antibodies against mab414 (second column, red) were used to visualize co-localization of SMPD4-GFP (first column, green) with nuclear pores during NE/NPC reassembly in telophase and anaphase ($n = 2$ experiments, $n > 5$ cells per experiment, scale bars = 1 μ m).

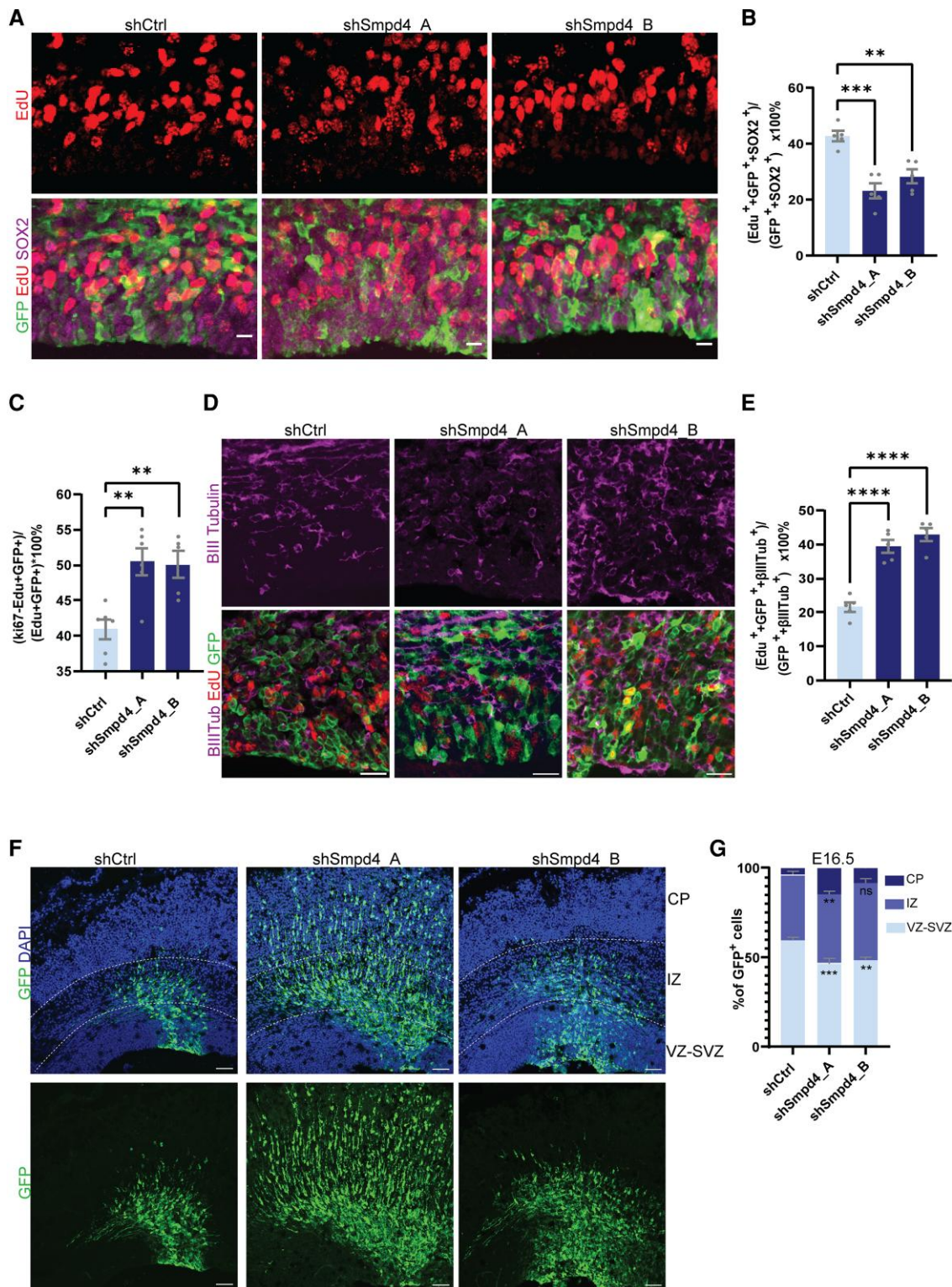


Figure 5 SMPD4 depletion in embryonic mice cortex affects apical progenitor proliferation and fate. (A and B) Immunostainings on cryosections of E16.5 mouse cortices, 48 h after electroporation, for GFP (green), EdU (top row, red) and SOX2 (magenta) to determine the percentage of proliferating apical progenitors (scale bars = 10 μ m, $n = 5-6$ brains, one-way ANOVA with Sidák post hoc test, $**P = 0.0018$, $***P = 0.0001$). (C) Quantification of triple immunostainings for GFP, Ki67 and EdU on shRNA electroporated cortices, performed to calculate the percentage of cells exiting the cell cycle at E16.5, 2 days after electroporation ($n = 5-6$ brains, one-way ANOVA with Sidák post hoc test, $**P = 0.0028$ shSmpd4_A versus ctrl, $**P = 0.0055$ shSmpd4_B versus ctrl). (D and E) Triple immunostainings for GFP, β III-Tubulin (top row, magenta) and EdU on shRNA electroporated cortices used to quantify the production of neuronal cells at E16.5, 2 days after electroporation (scale bars = 20 μ m, $n = 5$ brains, one-way ANOVA with Sidák post hoc test, $P = <0.0001$). (F and G) Distribution of shRNA-electroporated cells at E16.5, 48 h after electroporation (scale bars = 50 μ m, $n = 5$ brains, one-way ANOVA with Sidák post hoc test; VZ/SVZ: Ctrl versus shSmpd4_A3 $P = 0.0004$, Ctrl versus shSmpd4_B1 $P = 0.0020$; CP Ctrl versus shSmpd4_A3 $P = 0.0036$). Subdivisions of the cortical wall were made by nucleus density (DAPI) and are indicated with dashed lines: CP = cortical plate; IZ = intermediate zone; SVZ/VZ = subventricular zone/ventricular zone.

β III-Tubulin-positive cells compared to the shCtrl-targeted cells, indicating that the increased cell-cycle exit corresponds to premature differentiation (Fig. 5D and E; shCtrl: 21.6%; shSmpd4_A; 39.4% shSmpd4_B 42.9%). A disruption of neurogenesis has previously been associated with increased ER stress in apical progenitors.^{25,36} Therefore, we assessed the expression levels of the ER stress markers protein disulphide isomerase (PDI) and calreticulin in regions targeted by electroporation (GFP⁺). Supplementary Fig. 5D shows that the depletion of SMPD4 in these cortices did not result in upregulation of ER stress markers.

We next assessed whether the increased cell-cycle exit and premature neuronal differentiation had an impact in the migration of newborn projection neurons. The distribution of GFP-positive projection neurons was assessed throughout the cortex at E16.5. For this analysis, the cortical wall was subdivided into the subventricular zone (SVZ)/VZ, intermediate zone (IZ) and cortical plate (CP). At E16.5, knockdown of *Smpd4* resulted in a reduction in the fraction of GFP⁺ cells in the VZ/SVZ zone and a subsequent increase of GFP⁺ cells in the IZ and CP (Fig. 5F and G). Altogether, these *in vivo* results suggest that loss of SMPD4 activity promotes neurogenesis, apparent premature migration and may lead to a precocious exhaustion of apical progenitors, which is one core cellular pathophysiological defects underlying microcephaly.^{2,24,25}

Simultaneously, we attempted to study brain development in an *smpd4* mutant zebrafish model. Previous reports from our institute have shown the additional value of zebrafish models to study the effect of human pathogenic variants in poorly known genes on vertebrate brain development.^{26–29} However, after efficiently mutating out the single zebrafish SMPD4 homologue, the zebrafish *smpd4* LoF mutants did not recapitulate any of the structural or molecular defects described in humans or show other developmental or functional anomalies.

Discussion

The present study shows the importance of NE dynamics and neuronal sphingomyelinase activity for brain development and for the pathogenesis of microcephaly. We demonstrate that depletion of SMPD4, a low-abundance neutral sphingomyelinase, interferes with cell-cycle progression by decreasing cell proliferation rates and prolonging mitotic duration. These defects are paralleled by disturbances in NE dynamics and NPC insertion. Moreover, we show that this sphingomyelinase is essential to maintain the proliferating capacity of apical progenitors *in vivo* in the embryonic mammalian cortex, leading to premature neuronal differentiation and depletion of the progenitor pool.

The summary of all clinical features observed in published cases and the cases presented here shows that congenital progressive microcephaly and neurodevelopmental disorders are the most prevalent features related to LoF SMPD4 variants. All new subjects with SMPD4 variants described in this study and surviving beyond infancy presented with insulin-dependent diabetes, bringing the total percentage to 27%. This makes diabetes, sporadically reported in previous studies, the most common age-dependent feature of the SMPD4-related disorder besides neurological abnormalities and complications of IUGR/prematurity. This increase can be explained by the longer follow-up at older age of the less severely affected subjects (Family 1). The onset of diabetes occurred during puberty in most individuals. The majority of previously published individuals did not survive or did not reach this age by time of publication, explaining the lower incidence.

Insulin-dependent diabetes results from destruction of pancreatic beta-cells, which is often triggered by (auto)immune reactions. However, rare human mutations have shown that dysregulation of both the ER stress and the unfolded protein response contribute to the pathogenesis of insulin-dependent diabetes, as they also regulate beta-cell apoptosis.^{8–11,30} While we focused on NE membrane dynamics, SMPD4 is also known to localize to the ER and we have previously shown that its absence leads to signs of ER stress, apoptosis and increased autophagy in skin fibroblasts.⁴ To our knowledge, insulin-dependent diabetes has not been observed in individuals with variants in genes regulating NE homeostasis, while insulin-resistant type 2 diabetes has been described in laminopathy-related LMNB2 mutations, causing abnormally lobed interphase nuclei and other laminopathies like Dunnigan syndrome.³¹ In addition, the combination of microcephaly and diabetes has been described several times in children with variants in ER stress-related genes.^{8–11,30} We hypothesize that the insulin-dependent diabetes could be related to the function of SMPD4 in NE dynamics as well as to its function in the ER by causing susceptibility to apoptosis. We therefore recommend control of glucose metabolism in the diagnostic work-up and regular controls in the follow-up of subjects with SMPD4-related disorder.

A decrease in neuronal progenitor numbers during embryonic brain development is known to result in microcephaly. This decrease can be caused by dysregulation of the balance between symmetric and asymmetric divisions of apical progenitors. Symmetric divisions result in two apical progenitors, while asymmetric divisions result in one apical progenitor and one intermediate progenitor or a projection neuron.² Recent studies show that prolonged mitosis of neuronal progenitors alters neuronal cell fate by altering the balance between symmetric and asymmetric cell divisions and increasing apoptosis.^{24,32} We report that loss of SMPD4 prolongs mitosis in hNSCs and human SMPD4-deficient fibroblasts. We also show that in mouse embryos, loss of *Smpd4* resulted in an altered balance of neurogenic and proliferative progenitor cell divisions. Although we have not measured mitotic duration directly in embryonic mouse brain, the prolonged mitotic duration observed in SMPD4-depleted hNSCs provides a good explanation for this observation. Prolonged mitosis might not only interfere with the balance in progenitor cell divisions, but also impact the survival of neuronal progenitors.^{24,32} While SMPD4-depleted cells were more susceptible to undergo apoptosis upon hydrogen peroxide treatment, we did not observe increased cell death in cells with NE remodelling defects. Recent studies have shown that, in the pathogenesis of microcephaly, depletion of apical progenitors is not always associated with apoptosis.³³

The absence of SMPD4 interfered with normal NE disassembly and reassembly during mitosis. Moreover, it led to decreased insertion of new NPCs. While the importance of NE homeostasis and NPC biogenesis in the development of microcephaly has previously been suggested, the SMPD4-related disorder is the first human disease linked to the regulation of NE/NPC dynamics at the lipid level. Variants in NE protein ANKLE2 are related to microcephaly with simplified gyration, corpus callosum agenesis, cerebellar hypoplasia and skin pigmentation defects.³⁴ ANKLE2 regulates NE reassembly during mitotic exit and its depletion results in destabilization of the inner NE, with polylobed NE structures after mitosis, reminiscent of the SMPD4-related phenotype shown here. Variants in LMNB1, encoding for inner nuclear membrane lamin B1, disrupt NE integrity and nuclear lamina disassembly and result in severe congenital microcephaly with short stature, variable intellectual disability and epilepsy.³⁵ Also, variants in different NPC proteins

(NUP107, NUP37, NUP133, NUP188, NUP214) are related to microcephaly.^{36–40} Although the disease mechanisms underlying those disorders are not fully understood, we have previously shown, and we confirm here, that SMPD4 directly interacts with NPC components, which encourages investigation of the role of NPCs in the onset of microcephaly.

The involvement of NE dynamics in regulating cell division in neural progenitors has been studied with the depletion of Ankle2 in *Drosophila*, which results in disturbed NE morphology and altered asymmetric/symmetric cell division ratios in neural blasts.³⁴ Also ER stress is a mechanism known to disturb the balance between symmetric and asymmetric cell divisions.^{25,41} While loss of SMPD4 has been shown to result in ER stress signs *in vitro*, we did not observe upregulation of ER stress markers in the apical progenitors of embryonic mice. However, our observations took place in a limited time window and follow-up studies in transgenic animals could provide the answer to this question.

We show for the first time that fibroblasts with complete LoF variants in SMPD4 have a deficiency of SMPD4-specific TNF-stimulated nSMase activity. This observation is crucial to demonstrate that the protein coded by SMPD4 has in itself both an enzymatic activity and a lipid-regulating function. Interestingly, its loss does not alter the global lipidome, either in the total cell homogenate or in the nuclear subcellular fraction. These findings raise the possibility that SMPD4 is required for the regulation of local or transient changes in membrane lipid composition. Because ceramide production induces membrane curvature, it is possible that SMPD4 contributes to the formation of membrane curvature during NE reassembly and NPC insertion. The new NE initially forms from mitotic ER stacks that are recruited to chromatin. Afterwards, membrane-remodelling events occur to build a bilayer membrane with new NPCs inserted.¹⁵ Other membrane bending factors, such as RTN4, YOP1 and RET1, have been shown to be important for mitotic NE remodelling and NPC insertion.^{42–44} While further studies are needed to gain insight into the direct effect of SMPD4 on membrane remodelling, we hypothesize that the ceramides produced by SMPD4 contribute to NE reassembly and NPC insertion via the induction of membrane curvature.⁴⁵

NE breakdown is controlled by the phosphorylation of NE and NPC proteins. It is generally assumed that these phosphorylation events disrupt the interactions between NE or NPC components at the onset of mitosis.¹⁸ Large studies mapping mitotic phosphorylation sites found SMPD4 to be one of the proteins that becomes phosphorylated during mitosis.^{46,47} This phosphorylation step may disrupt the interactions with other NE components, but could also regulate the enzymatic activity of SMPD4 during mitosis. While the role of NE lipid metabolism during NE breakdown is poorly explored, it is suggested that membrane remodelling factors and lipid-metabolizing enzymes are recruited to the centrosome during the onset of the breakdown.¹⁵ Interestingly, we observed relocalization of SMPD4 to the regions surrounding the centrosomes in early prophase. During this cell-cycle phase, the centrosome is tethered to the NE to regulate breakdown and is thought to serve as a regional hub to direct modelling of the NE.

Altogether, we show that loss of neutral sphingomyelinase-3 (SMPD4) not only results in a severe developmental disorder with microcephaly, but also causes age-related insulin-dependent diabetes. Our results show the importance of this sphingomyelinase in maintenance of the neuronal progenitor pool and regulation of cell-cycle exit during embryonic cortical development. At the cellular level, our results provide new mechanistic insights into the role of sphingolipid metabolism during mitotic NE remodelling, NPC

insertion and mitotic progression. Follow-up studies that investigate the biochemical properties of SMPD4-depleted membranes will provide information about the direct effects of sphingolipid metabolism on membrane properties and membrane dynamics. This could also provide additional insights into the role of other lipids during NE breakdown, NE reassembly and NPC insertion and their potential contribution to human disease. Our results confirm that variants in genes regulating NE homeostasis, NPC insertion and/or mitotic progression should be considered in patients with severe progressive microcephaly.

Acknowledgements

We thank the patients and their families for participation in this study. We thank Dr Maarten Fornerod and Dr Niels Galjart for fruitful discussions and their support.

Funding

G.M.S.M. is supported by ZonMW Top grant #91217045. D.J.S is supported by an EMBO fellowship #8857.

Competing interests

The authors report no competing interests.

Supplementary material

Supplementary material is available at *Brain* online.

References

1. Siskos N, Stylianopoulou E, Skavdis G, Grigoriou ME. Molecular genetics of microcephaly primary hereditary: An overview. *Brain Sci.* 2021;11:581.
2. Jayaraman D, Bae BI, Walsh CA. The genetics of primary microcephaly. *Annu Rev Genomics Hum Genet.* 2018;19:177–200.
3. Passemard S, Perez F, Gressens P, El Ghouzzi V. Endoplasmic reticulum and Golgi stress in microcephaly. *Cell Stress.* 2019;3:369–384.
4. Magini P, Smits DJ, Vandervore L, et al. Loss of SMPD4 causes a developmental disorder characterized by microcephaly and congenital arthrogryposis. *Am J Hum Genet.* 2019;105:689–705.
5. Ravenscroft G, Clayton JS, Faiz F, et al. Neurogenetic fetal akinesia and arthrogryposis: Genetics, expanding genotype–phenotypes and functional genomics. *J Med Genet.* 2021;58:609–618.
6. Yamada M, Suzuki H, Shima T, Uehara T, Kosaki K. A patient with compound heterozygosity of SMPD4: Another example of utility of exome-based copy number analysis in autosomal recessive disorders. *Am J Med Genet A.* 2022;188:613–617.
7. Bijarnia-Mahay S, Somashekar PH, Kaur P, et al. Growth and neurodevelopmental disorder with arthrogryposis, microcephaly and structural brain anomalies caused by bi-allelic partial deletion of SMPD4 gene. *J Hum Genet.* 2022;67:133–136.
8. Abdel-Salam GM, Schaffer AE, Zaki MS, et al. A homozygous IER3IP1 mutation causes microcephaly with simplified gyral pattern, epilepsy, and permanent neonatal diabetes syndrome (MEDS). *Am J Med Genet A.* 2012;158A:2788–2796.
9. Poulton CJ, Schot R, Kia SK, et al. Microcephaly with simplified gyration, epilepsy, and infantile diabetes linked to

- inappropriate apoptosis of neural progenitors. *Am J Hum Genet.* 2011;89:265–276.
10. Skopkova M, Hennig F, Shin BS, et al. EIF2S3 Mutations associated with severe X-linked intellectual disability syndrome MEHMO. *Hum Mutat.* 2017;38:409–425.
 11. Senee V, Vattem KM, Delepine M, et al. Wolcott-Rallison syndrome: Clinical, genetic, and functional study of EIF2AK3 mutations and suggestion of genetic heterogeneity. *Diabetes.* 2004;53:1876–1883.
 12. Mansfeld J, Guttinger S, Hawryluk-Gara LA, et al. The conserved transmembrane nucleoporin NDC1 is required for nuclear pore complex assembly in vertebrate cells. *Mol Cell.* 2006;22:93–103.
 13. Stavru F, Hulsmann BB, Spang A, Hartmann E, Cordes VC, Görlich D. NDC1: A crucial membrane-integral nucleoporin of metazoan nuclear pore complexes. *J Cell Biol.* 2006;173:509–519.
 14. Cronshaw JM, Krutchinsky AN, Zhang W, Chait BT, Matunis MJ. Proteomic analysis of the mammalian nuclear pore complex. *J Cell Biol.* 2002;158:915–927.
 15. Guttinger S, Laurell E, Kutay U. Orchestrating nuclear envelope disassembly and reassembly during mitosis. *Nat Rev Mol Cell Biol.* 2009;10:178–191.
 16. Burke B, Shanahan C, Salina D, Crisp M. Aspects of nuclear envelope dynamics in mitotic cells. *Novartis Found Symp.* 2005;264:22–30; discussion 30–4, 227–30.
 17. Burke B, Crisp M, Salina D. Nuclear envelope dynamics during mitosis. *Symp Soc Exp Biol.* 2004;56:205–216.
 18. Linder MI, Kohler M, Boersema P, et al. Mitotic disassembly of nuclear pore complexes involves CDK1- and PLK1-mediated phosphorylation of key interconnecting nucleoporins. *Dev Cell.* 2017;43:141–156.e7.
 19. Wohler E, Martin R, Griffith S, et al. PhenoDB, GeneMatcher and VariantMatcher, tools for analysis and sharing of sequence data. *Orphanet J Rare Dis.* 2021;16:365.
 20. Vandervore LV, Schot R, Milanese C, et al. TMX2 is a crucial regulator of cellular redox state, and its dysfunction causes severe brain developmental abnormalities. *Am J Hum Genet.* 2019;105:1126–1147.
 21. Moylan JS, Smith JD, Wolf Horrell EM, et al. Neutral sphingomyelinase-3 mediates TNF-stimulated oxidant activity in skeletal muscle. *Redox Biol.* 2014;2:910–920.
 22. Quintern LE, Sandhoff K. Human acid sphingomyelinase from human urine. *Methods Enzymol.* 1991;197:536–540.
 23. Krut O, Wiegmann K, Kashkar H, Yazdanpanah B, Krönke M. Novel tumor necrosis factor-responsive mammalian neutral sphingomyelinase-3 is a C-tail-anchored protein. *J Biol Chem.* 2006;281:13784–13793.
 24. Mitchell-Dick A, Chalem A, Pilaz LJ, Silver DL. Acute lengthening of progenitor mitosis influences progeny fate during cortical development in vivo. *Dev Neurosci.* 2019;41(5–6):300–317.
 25. Laguesse S, Creppe C, Nedialkova DD, et al. A dynamic unfolded protein response contributes to the control of cortical neurogenesis. *Dev Cell.* 2015;35:553–567.
 26. Berdowski WM, van der Linde HC, Breur M, et al. Dominant-acting CSF1R variants cause microglial depletion and altered astrocytic phenotype in zebrafish and adult-onset leukodystrophy. *Acta Neuropathol.* 2022;144:211–239.
 27. Kuil LE, Lopez Marti A, Carreras Mascaro A, et al. Hexb enzyme deficiency leads to lysosomal abnormalities in radial glia and microglia in zebrafish brain development. *Glia.* 2019;67:1705–1718.
 28. Sanderson LE, Lanko K, Alsagob M, et al. Bi-allelic variants in HOPS complex subunit VPS41 cause cerebellar ataxia and abnormal membrane trafficking. *Brain.* 2021;144:769–780.
 29. Perenthaler E, Nikoncuk A, Yousefi S, et al. Loss of UGP2 in brain leads to a severe epileptic encephalopathy, emphasizing that bi-allelic isoform-specific start-loss mutations of essential genes can cause genetic diseases. *Acta Neuropathol.* 2020;139:415–442.
 30. De Franco E, Lytrivi M, Ibrahim H, et al. YIPF5 mutations cause neonatal diabetes and microcephaly through endoplasmic reticulum stress. *J Clin Invest.* 2020;130:6338–6353.
 31. Varlet AA, Desgrouas C, Jebane C, et al. A rare mutation in LMNB2 associated with lipodystrophy drives premature cell senescence. *Cells.* 2021;11:50.
 32. Pilaz LJ, McMahon JJ, Miller EE, et al. Prolonged mitosis of neural progenitors alters cell fate in the developing brain. *Neuron.* 2016;89:83–99.
 33. Carpentieri JA, Di Cicco A, Lampic M, et al. Endosomal trafficking defects alter neural progenitor proliferation and cause microcephaly. *Nat Commun.* 2022;13:16.
 34. Link N, Chung H, Jolly A, et al. Mutations in ANKLE2, a ZIKA virus target, disrupt an asymmetric cell division pathway in *Drosophila* neuroblasts to cause microcephaly. *Dev Cell.* 2019;51:713–729.e6.
 35. Cristofoli F, Moss T, Moore HW, et al. De novo variants in LMNB1 cause pronounced syndromic microcephaly and disruption of nuclear envelope integrity. *Am J Hum Genet.* 2020;107:753–762.
 36. Sandestig A, Engstrom K, Pepler A, et al. NUP188 biallelic loss of function may underlie a new syndrome: Nucleoporin 188 insufficiency syndrome? *Mol Syndromol.* 2020;10:313–319.
 37. Rosti RO, Sotak BN, Bielas SL, et al. Homozygous mutation in NUP107 leads to microcephaly with steroid-resistant nephrotic condition similar to Galloway–Mowat syndrome. *J Med Genet.* 2017;54:399–403.
 38. Muir AM, Cohen JL, Sheppard SE, et al. Bi-allelic loss-of-function variants in NUP188 cause a recognizable syndrome characterized by neurologic, ocular, and cardiac abnormalities. *Am J Hum Genet.* 2020;106:623–631.
 39. Fujita A, Tsukaguchi H, Koshimizu E, et al. Homozygous splicing mutation in NUP133 causes Galloway–Mowat syndrome. *Ann Neurol.* 2018;84:814–828.
 40. Fichtman B, Harel T, Biran N, et al. Pathogenic variants in NUP214 cause “plugged” nuclear pore channels and acute febrile encephalopathy. *Am J Hum Genet.* 2019;105:48–64.
 41. Gladwyn-Ng I, Cordón-Barris L, Alfano C, et al. Stress-induced unfolded protein response contributes to Zika virus-associated microcephaly. *Nat Neurosci.* 2018;21:63–71.
 42. Dawson TR, Lazarus MD, Hetzer MW, Wente SR. ER membrane-bending proteins are necessary for de novo nuclear pore formation. *J Cell Biol.* 2009;184:659–675.
 43. Hu J, Shibata Y, Voss C, et al. Membrane proteins of the endoplasmic reticulum induce high-curvature tubules. *Science.* 2008;319:1247–1250.
 44. Kiseleva E, Morozova KN, Voeltz GK, Allen TD, Goldberg MW. Reticulon 4a/NogoA locates to regions of high membrane curvature and may have a role in nuclear envelope growth. *J Struct Biol.* 2007;160:224–235.
 45. Peeters BWA, Piet ACA, Fornerod M. Generating membrane curvature at the nuclear pore: A lipid point of view. *Cells.* 2022;11:469.
 46. Kettenbach AN, Schweppe DK, Faherty BK, Pechenick D, Pletnev AA, Gerber SA. Quantitative phosphoproteomics identifies substrates and functional modules of Aurora and polo-like kinase activities in mitotic cells. *Sci Signal.* 2011;4:rs5.
 47. Olsen JV, Vermeulen M, Santamaria A, et al. Quantitative phosphoproteomics reveals widespread full phosphorylation site occupancy during mitosis. *Sci Signal.* 2010;3:ra3.